

Simulating self-avoiding walks in bounded domains

Tom Kennedy
 Department of Mathematics
 University of Arizona
 Tucson, AZ 85721
 email: tgk@math.arizona.edu

April 10, 2018

Abstract

Let D be a domain in the plane containing the origin. We are interested in the ensemble of self-avoiding walks (SAW's) in D which start at the origin and end on the boundary of the domain. We introduce an ensemble of SAW's that we expect to have the same scaling limit. The advantage of our ensemble is that it can be simulated using the pivot algorithm. Our ensemble makes it possible to accurately study SLE predictions for the SAW in bounded simply connected domains. One such prediction is the distribution along the boundary of the endpoint of the SAW. We use the pivot algorithm to simulate our ensemble and study this density. In particular the lattice effects in this density that persist in the scaling limit are seen to be given by a purely local function.

1 Introduction

In two dimensions there has been a lot of interest in the self-avoiding walk (SAW) in simply connected domains D because of its conjectured relationship with SLE. One is interested in two cases: the radial case in which the SAW starts at a point inside the domain and ends on the boundary and the chordal case in which it starts and ends at boundary points. If one fixes the starting and ending points then Lawler, Schramm and Werner conjectured that the scaling limit is radial or chordal $\text{SLE}_{8/3}$ [7]. If one fixes the starting point but allows all SAW's that end anywhere on the boundary, then there are conjectures for the hitting density along the boundary from SLE partition functions [7, 6]. Some progress towards proving the conformal invariance of the SAW was made by Duminil-Copin and Smirnov [2].

For the SAW in the full plane or a half plane there is a very fast Monte Carlo algorithm known as the pivot algorithm. (Clisby's recent implementation of the algorithm using binary trees has dramatically increased its speed [1].) However the pivot algorithm cannot be used for

the SAW in a bounded domain. The pivoting will almost always produce a SAW that does not end on the boundary of the domain or leaves the domain. And the pivot algorithm works on an ensemble of SAW's with a fixed number of steps. For the SAW in D we must allow SAW's with all numbers of steps.

In this paper we show how to use the pivot algorithm to simulate an ensemble of SAW's that should have the same scaling limit as the ensemble of SAW's in D that end on the boundary. The key idea is to consider the ensemble of all SAW's starting at the origin such that there is a positive constant $\lambda > 0$ such that the SAW stays in the dilated domain λD and ends on the boundary of λD . We refer to this ensemble as the "dilation ensemble." The SAW's in the dilation ensemble have an arbitrary number of steps. Nonetheless we will argue that in the scaling limit this ensemble can be realized using the ensemble of walks with a fixed number of steps that satisfy the constraint above. This allows us to use the pivot algorithm to simulate the scaling limit of the ensemble.

If one allows the SAW to end anywhere on the boundary of the domain, then in the scaling limit the distribution of the endpoint along the boundary gives a probability measure on the boundary analogous to harmonic measure for the ordinary random walk. Assuming the boundary is smooth, the distribution should be absolutely continuous with respect to arc length along the boundary. Lawler, Schramm and Werner have given an explicit conjecture for this boundary density [7] using SLE partition functions. The simplest description of their conjecture is that the boundary density for the SAW is proportional to the density for harmonic measure raised to the $5/8$ power. In [7] they considered domains in which the sides are parallel to a lattice direction. In the case of a horizontal strip with the SAW starting on one boundary of the strip and ending on the other boundary, the conjecture for the boundary density was tested in [3], and good agreement was found. The conjecture was discussed further by Lawler in [6] where it was stated for general simply connected domains "after taking care of the local lattice effects."

In [5] it was conjectured that the local lattice effect at a point z on the boundary only depends on the angle of the tangent to the boundary at z . There are a variety of ways to interpret what it means for the SAW which is on a lattice to end on the boundary of D which typically does not pass through lattice sites. The precise nature of the lattice effects depends on which interpretation is used. Explicit conjectures for these local lattice effects were given in [5] for two particular interpretations of ending on the boundary. In one interpretation one considers all SAW's ω with $\omega(i) \in D$ for $i < |\omega|$ and $\omega(|\omega|) \notin D$, where $|\omega|$ is the number of steps in the SAW. While this is one of the most natural interpretations, there is no good algorithm for simulating this ensemble. The other ensemble considered in [5] is the "cut-curve" ensemble. It uses infinite length SAW's in the full plane and conditions on the event that the SAW crosses the boundary of D only once. (In practice we use SAW's with a fixed length N and take N large enough that the typical size of the SAW is much larger than the domain D .) SAW's in this ensemble are equivalent to the concatenation of a SAW in D from the origin to the boundary of D and a SAW in the exterior of D , starting at the same boundary point and going to ∞ .

One can use the pivot algorithm to simulate the "cut-curve" ensemble. But this has the

disadvantage that one must deal with a double limit - one must first let the number of steps in the SAW go to infinity and then take the lattice spacing to zero. In practice this means that one must simulate SAW's that are much larger than the domain D . So such simulations are less efficient than the method we will introduce for the dilation ensemble.

In the next section we define the dilation ensemble and show how it may be simulated using the pivot algorithm on the ensemble of walks with a fixed number of steps. In section three we give an explicit conjecture for the lattice effects in our dilation ensemble and show how these effects may be computed by simulation. In section four we use our method for simulating the dilation ensemble to study the SAW in several different domains. We compare the boundary densities we find with the SLE partition function predictions for these densities.

2 The dilation ensemble

We first consider the radial case. We assume that our simply connected domain D contains the origin and has a boundary which is a smooth curve which we denote by ∂D . We also assume that the domain is star-shaped with respect to the origin, i.e., any ray from the origin intersects ∂D in only one point. (It would be interesting to generalize our approach to domains that do not have this property.) We are interested in the ensemble of SAW's that start at the origin and end on ∂D . Note that we are not fixing the point on the boundary where the SAW must end; the endpoint of the SAW is a random point on the boundary.

The dilation ensemble can be described as all SAW's such that the domain D can be dilated so that the SAW lies in the dilated domain and ends on the boundary of the dilated domain. We let $\delta > 0$ denote the lattice spacing. We start with the ensemble of all SAW's in the full plane on the lattice $\delta\mathbb{Z}^2$ that start at the origin with any finite number of steps. For a SAW ω we let $|\omega|$ denote the number of steps in the walk. The walk ω is given the weight $\mu^{-|\omega|}$ where μ is the connective constant. (It is given by $\mu = \lim_{N \rightarrow \infty} c_N^{1/N}$ where c_N denotes the number of SAW's in the full plane with N steps that start at 0. The existence of this limit follows from the subadditivity of $\ln(c_N)$ [8].) We will impose two constraints on the ensemble of all finite length SAW's. We let $\lambda(\omega) > 0$ be the dilation such that the endpoint of ω is on the dilated curve $\lambda(\omega)\partial D$. The partition function for the ensemble of all finite length SAW's starting at the origin is infinite, so we add the constraint that $\lambda(\omega)$ lies in $[\lambda_1, \lambda_2]$ where $\lambda_1 < \lambda_2$ are positive constants. We expect that this makes the partition function finite, although we cannot prove this. The walk ω ends on the curve $\lambda(\omega)\partial D$, but it need not stay inside the region $\lambda(\omega)D$. Our second constraint is that the walk ω does stay strictly inside this region except for the endpoint. We let $1_D(\omega)$ denote the indicator function that is 1 if ω stays strictly inside this region except for its endpoint and 0 if it does not. So our ensemble corresponds to the partition function

$$Z = \sum_{\omega} \mu^{-|\omega|} 1_D(\omega) 1(\lambda_1 \leq \lambda(\omega) \leq \lambda_2) W(\omega) \quad (1)$$

We have included a weighting factor $W(\omega)$ which we will define later to make our ensemble correspond to the ensemble of SAW's in D that end on the boundary. Associated with this

partition function is a probability measure on simple curves in D that end on the boundary. Let $\psi(\gamma)$ be a function on simple curves γ in D that start at the origin and end on ∂D . If $1_D(\omega) = 1$, then $\frac{\omega}{\lambda(\omega)}$ is such a curve and so $\psi(\frac{\omega}{\lambda(\omega)})$ is defined. Define

$$Z(\psi) = \sum_{\omega} \mu^{-|\omega|} 1_D(\omega) 1(\lambda_1 \leq \lambda(\omega) \leq \lambda_2) W(\omega) \psi\left(\frac{\omega}{\lambda(\omega)}\right) \quad (2)$$

The expected value of ψ is defined to be $Z(\psi)/Z$. (Both Z and $Z(\psi)$ depend on λ_1 and λ_2 , but they will be fixed throughout our discussion.)

We now consider how this ensemble corresponds to the ensemble of SAW's in D that end on ∂D . For a large integer N , let $d\lambda = (\lambda_2 - \lambda_1)/N$. We think of the region between the curves $\lambda_1\partial D$ and $\lambda_2\partial D$ as the union of the regions between the curves $(\lambda_1 + (k-1)d\lambda)\partial D$ and $(\lambda_1 + kd\lambda)\partial D$ where $k = 1, 2, \dots, N$. In the scaling limit, the ensembles corresponding to these different regions are related by just a dilation. So they will all give the same expected value to ψ . The region between $(\lambda_1 + (k-1)d\lambda)\partial D$ and $(\lambda_1 + kd\lambda)\partial D$ corresponds to thickening the boundary of $(\lambda_1 + kd\lambda)\partial D$. So we can think of the dilation ensemble as interpreting the constraint that the SAW stays in D and ends on ∂D as thickening the boundary.

It is important to observe that the way that our ensemble thickens the boundary is not uniform along ∂D . The natural way to thicken the curve would be to take the thickness in the direction perpendicular to the curve to be constant along the curve. Let $\rho(z)$ denote the density of the endpoint of the SAW in D which ends on the boundary. In the dilation ensemble if we take the weight $W(\omega)$ to just be constant, then the corresponding boundary density will be proportional to $\rho(z)$ times the thickness at z . To correct for this we take $W(\omega)$ to be proportional to the inverse of this thickness.

Recall that we assume that our domain is star-shaped with respect to the origin, i.e., any ray from the origin intersects ∂D in exactly one point. So we can parametrize ∂D by the polar angle θ with respect to the origin. We let $D(\theta)$ be the distance from the origin to the curve in the direction θ . Along the ray at polar angle θ the thickness is $(\lambda + d\lambda)D(\theta) - \lambda D(\theta) = D(\theta)d\lambda$. But this segment is not perpendicular to the tangent line. Let $\alpha(\theta)$ be the angle of a line perpendicular to ∂D at our point. Then the thickness of our shell perpendicular to the tangent line is $D(\theta) \cos(\theta - \alpha(\theta))$. Thus we define

$$W(\omega) = [D(\theta(\omega)) \cos(\theta(\omega) - \alpha(\theta(\omega)))]^{-1} \quad (3)$$

where $\theta(\omega)$ is the polar angle of the endpoint of ω . Note that the weight only depends on the polar angle of the endpoint of ω .

The dilation ensemble (1) includes SAW's of all lengths. To simulate it using the pivot algorithm we must relate it to the ensemble of SAW's with a fixed length in which each SAW has the same weight. Our method for doing this is closely related to the method in [4] for relating the ensemble of SAW's in the half-plane with a fixed number of steps to radial SLE. We decompose the sum in $Z(\psi)$, as defined in (2), according to the length of ω .

$$Z(\psi) = \sum_n \mu^{-n} \sum_{\omega:|\omega|=n} 1_D(\omega) 1(\lambda_1 \leq \lambda(\omega) \leq \lambda_2) W(\omega) \psi\left(\frac{\omega}{\lambda(\omega)}\right)$$

Let c_n be number of SAW in the full plane starting at 0 with n steps. We have

$$Z(\psi) = \sum_n c_n \mu^{-n} \frac{1}{c_n} \sum_{\omega: |\omega|=n} 1_D(\omega) 1(\lambda_1 \leq \lambda(\omega) \leq \lambda_2) W(\omega) \psi\left(\frac{\omega}{\lambda(\omega)}\right)$$

The constraint $\lambda(\omega) \geq \lambda_1$ implies that ω must have at least λ_1/δ steps. So as the lattice spacing goes to zero, the first n for which the summand in the sum on n is nonzero goes to infinity. Since c_n is asymptotic to $\mu^n n^{\gamma-1}$, we replace $c_n \mu^{-n}$ by $n^{\gamma-1}$. Let P_n be the uniform probability measure on all SAW's starting at the origin with n steps, and let E_n be the associated expected value. Then we can write the above as

$$Z(\psi) = \sum_n n^{\gamma-1} E_n[1_D(\omega) 1(\lambda_1 \leq \lambda(\omega) \leq \lambda_2) W(\omega) \psi\left(\frac{\omega}{\lambda(\omega)}\right)]$$

As noted before, the constraint $\lambda(\omega) \geq \lambda_1$ implies that the sum on n is only over large values. So we should be able to approximate E_n by its scaling limit. The constraint $1_D(\omega)$ is a bit tricky in the scaling limit, so we proceed as follows. Fix a large positive integer N . If n is also large and ω and γ are drawn from P_n and P_N , respectively, then the distributions of $\delta^{-1}n^{-\nu}\omega$ and $\delta^{-1}N^{-\nu}\gamma$ are approximately the same. So we will replace E_n by E_N by replacing $\delta^{-1}n^{-\nu}\omega$ by $\delta^{-1}N^{-\nu}\gamma$, i.e., we replace ω by $n^\nu N^{-\nu}\gamma$. So $\lambda(\omega)$ becomes $\lambda(n^\nu N^{-\nu}\gamma) = n^\nu N^{-\nu}\lambda(\gamma)$. Our weight $W(\omega)$ only depends on the polar angle of the endpoint of ω , so we can replace $W(\omega)$ by $W(\gamma)$. And we can replace $\psi\left(\frac{\omega}{\lambda(\omega)}\right)$ by $\psi\left(\frac{\gamma}{\lambda(\gamma)}\right)$.

The constraint $1_D(\omega)$ is more subtle. The probability that an n -step SAW stays on one side of a half plane is conjectured to go to zero as $n^{-\rho}$ as $n \rightarrow \infty$ with $\rho = 25/64$ [7]. So we expect that the probability that $1_D(\omega) = 1$ also goes to zero as $n^{-\rho}$. So we approximate $n^\rho 1_D(\omega)$ with $N^\rho 1_D(\gamma)$, i.e., we replace $1_D(\omega)$ by $N^\rho n^{-\rho} 1_D(\gamma)$. We now have

$$Z(\psi) \approx N^\rho \sum_n n^{\gamma-1-\rho} E_N[1_D(\gamma) 1(\lambda_1 \leq n^\nu N^{-\nu}\lambda(\gamma) \leq \lambda_2) W(\gamma) \psi\left(\frac{\gamma}{\lambda(\gamma)}\right)]$$

The n dependent part of this is

$$\sum_n n^{\gamma-1-\rho} 1(\lambda_1 \leq n^\nu N^{-\nu}\lambda(\gamma) \leq \lambda_2)$$

Since the constraint restricts the sum to large values of n , $n^{\gamma-1-\rho}$ is slowly varying and so we can think of this as a Riemann sum approximation to

$$\int_0^\infty x^{\gamma-1-\rho} 1(\lambda_1 \leq x^\nu N^{-\nu}\lambda(\gamma) \leq \lambda_2) dx = c N^{\gamma-\rho} [\lambda(\gamma)]^{(\rho-\gamma)/\nu}$$

where the constant c depends on λ_1 and λ_2 , but nothing else. Thus

$$Z(\psi) \approx c N^{\gamma-\rho} E_N[\lambda(\gamma)^{(\rho-\gamma)/\nu} 1_D(\gamma) W(\gamma) \psi\left(\frac{\gamma}{\lambda(\gamma)}\right)]$$

By taking $\psi = 1$, this result also gives an expression for Z .

The above derivation was for the radial case in which the starting point of the SAW is in the interior of D . If we take a domain which has the origin on its boundary and consider SAW's which start at the origin, stay in D and end on its boundary, then we can repeat the above derivation. The one important difference is that the number of walks c_n should now grow like $\mu^n n^{\gamma-1-\rho}$, rather than $\mu^n n^{\gamma-1}$. So the appropriate power for $\lambda(\gamma)$ becomes $p = \frac{2\rho-\gamma}{\nu}$.

We conjecture that when we take the scaling limit our approximations become exact. More precisely, we make the following conjecture.

Conjecture : *Let D be a simply connected domain which contains the origin (radial case) or has the origin on its boundary (chordal case), and which is star shaped with respect to the origin. Let ψ be a function on simple curves in D which start at the origin and end on the boundary. Let $Z(\psi)/Z$ be the expected value of ψ in the dilation ensemble of SAW's on a lattice of spacing δ as defined by (2). Let E_N be the uniform probability measure on N -step SAW's γ starting at the origin in the half plane (chordal case) or in the full plane (radial case). Let $\lambda(\gamma) > 0$ be such that γ ends on $\lambda(\gamma)\partial D$. Let $1_D(\gamma)$ be the indicator function of the event that γ is inside the domain $\lambda(\gamma)D$ except for its endpoint(s). Define the weight $W(\gamma)$ by (3). Then*

$$\lim_{\delta \rightarrow 0} \frac{Z(\psi)}{Z} = \lim_{N \rightarrow \infty} \frac{E_N[\lambda(\gamma)^p 1_D(\gamma) W(\gamma) \psi(\frac{\gamma}{\lambda(\gamma)})]}{E_N[\lambda(\gamma)^p 1_D(\gamma) W(\gamma)]} \quad (4)$$

$$p = \frac{\rho - \gamma}{\nu} = -61/48 \quad (\text{radial case}),$$

$$p = \frac{2\rho - \gamma}{\nu} = -3/4 \quad (\text{chordal case}).$$

3 Lattice effects in boundary densities

We expect that in the scaling limit the endpoint of the SAW on the boundary of the domain D will have a distribution that is absolutely continuous with respect to arc length along the boundary. We denote this boundary density by ρ . If we consider ordinary random walks instead of self-avoiding walks, then in the scaling limit this boundary distribution would be harmonic measure.

Let f be a conformal map on D . Then it is expected that the boundary density transforms as

$$\rho_D(z) = c|f'(z)|^{5/8} \rho_{f(D)}(f(z)), \quad z \in \partial D \quad (5)$$

except for a local lattice effect that persists in the scaling limit. If we take g to be the conformal map of D onto the unit disc that fixes the origin, then the above implies that $\rho_D(z)$ is proportional to $|g'(z)|^{5/8}$. Note that the conformal invariance of harmonic measure implies that the

boundary density for the ordinary random walk transforms in an analogous way except that the power of 5/8 is replaced by 1. Consequently (5) implies that the boundary density for the SAW is proportional to the boundary density for the ordinary random walk raised to the 5/8 power.

We now turn to the computation of the lattice effect correction to the boundary density. This computation for the dilation ensemble is analogous to what was done in [5]. The constraint that the SAW ω stays inside the dilated curve $\lambda(\omega)\partial D$ has both a macroscopic and microscopic nature. The conjecture (5) is the result of the macroscopic effect. Near the endpoint of the walk there is an additional microscopic effect. Consider a SAW that ends at z and consider the tangent line to the curve ∂D at z . The constraint that the SAW stays inside $\lambda(\omega)D$ implies that near the endpoint the SAW must stay on one side of this line. This will produce a factor $l(\theta)$ that depends on the angle of the tangent line with respect to the lattice.

For an angle θ , let L be the line with polar angle θ passing through the origin. We consider walks with N steps starting at the origin. Let c_N be the number of such walks, and let $b_N(\theta)$ be the number of such walks that stay on one side of the line. So $b_N(\theta)/c_N$ is the probability that an N step SAW stays on one side of the line. We expect that this probability goes to zero as $N^{-\rho}$ as $N \rightarrow \infty$, and we conjecture that the lattice effect function is given by

$$l(\theta) = \lim_{N \rightarrow \infty} \frac{b_N(\theta)}{c_N} N^\rho \quad (6)$$

Since θ and $\theta + 180$ give the same line, $l(\theta)$ has period 180 degrees. The function will have more symmetries depending on the type of lattice. For example, for the square lattice $l(\theta)$ has period 90 degrees and $l(\theta) = l(90 - \theta)$. If we use the weight $W(\omega)$ in (1) and (2), then the boundary density for the dilation ensemble will be $\rho_D(z)l(\theta(\omega))$ where $\theta(\omega)$ the polar angle of the endpoint of ω . To remove this lattice effect from our dilation ensemble we replace the weight $W(\omega)$ given by (3) by

$$\hat{W}(\omega) = \frac{W(\omega)}{l(\theta(\omega))} \quad (7)$$

In our conjecture (4) the weight $W(\omega)$ is used in both sides of this equation. The same derivation shows that this equality should also hold if we use $\hat{W}(\omega)$ in both sides.

We take the constraint that ω stays inside $\lambda(\omega)D$ to mean that it stays strictly inside the curve except for the endpoint. The other convention would be to allow ω to have sites that lie on $\lambda(\omega)\partial D$ in addition to its endpoint. If ∂D has flat sections, then there can be a big difference between these two conventions for angles θ such that a line through the origin at angle θ passes through some lattice sites. This will be the case for the equilateral triangle that we consider in our simulations.

In figure 1 we plot the lattice effect function $l(\theta)$ for the dilation ensemble and for two other ensembles, all on the square lattice. One is the cut-curve ensemble studied in [5]. The other ensemble is the “natural” ensemble in which we take all SAW’s such that all the sites on the

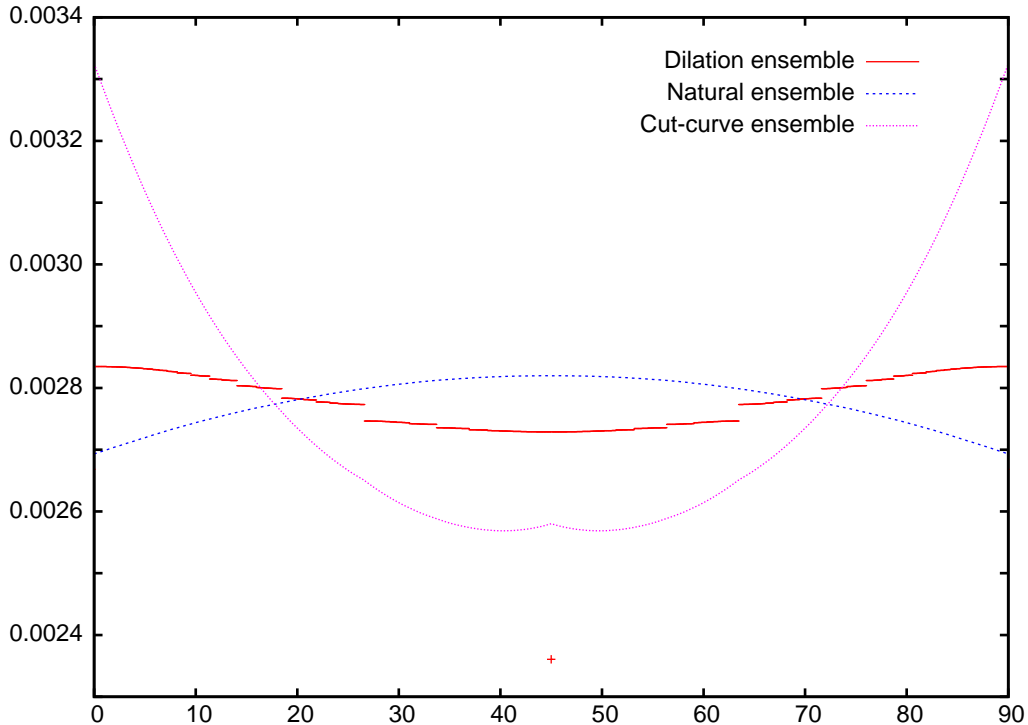


Figure 1: The lattice effect function $l(\theta)$ for three different ensembles on the square lattice.

walk are in D except for the endpoint which is outside of D . In other words, the last bond of the walk crosses the boundary of D and is the only bond which does so. All three functions have been normalized so that the total area under each curve is 1. It is important to note that the vertical scale of the plot does not include 0. These functions are actually relatively flat. Note that the lattice effect function for the dilation ensemble studied in this paper is considerably flatter than the function for the cut-curve ensemble that was simulated in [5].

The function $l(\theta)$ is continuous for the cut-curve and natural ensembles, but for the dilation ensemble it is not. For the square lattice it is discontinuous at θ such that $\tan(\theta)$ is rational. The biggest discontinuity is at $\theta = 0$, but it cannot be seen in the figure since $l(0) = 0.001516$ which is well below the region plotted. The second biggest discontinuity at $\theta = 45$ is seen in the figure as an isolated point at $l(45) = 0.002361$. This discontinuity is atypical in that $l(45-) = l(45+)$. Other discontinuities with $l(\theta-) \neq l(\theta+)$ can be seen in the figure. To see why $l(\theta)$ is discontinuous, consider the case of $\theta = 0$. Recall that we make the convention that the walk must stay strictly inside the domain except for the endpoint. So when θ is exactly 0, $b_N(\theta)$ counts walks that start at the origin and then stay strictly on one side of the horizontal axis. So the walk cannot visit any site on the horizontal axis. Now consider a θ that is slightly greater than zero and consider a walk which stays above this line. The sites on the negative horizontal axis are now above the line and so the walk can visit these sites. Thus $b_N(0)$ is

significantly smaller than $b_N(0^+)$. If we change the convention that the SAW must stay strictly inside the domain to allow SAW's that visit sites on the boundary, then the values at the angles where $l(\theta)$ is discontinuous will change but it will still be discontinuous.

4 Simulations

We use our conjecture to simulate the dilation ensemble and compare the boundary density found in the simulation with the density given by (5). Note that our simulations are testing three different conjectures. One is the conjecture (4) that says we can use the fixed length ensemble to simulate the ensemble of SAW's in a bounded domain. Another is the SLE partition function prediction for the boundary density (5). And finally there is the conjecture that the lattice effect correction to this density is given by $l(\theta)$, i.e., by using the weight (7).

The exact predictions for the boundary density from SLE partition functions (5) are given in the appendix. In our simulations we work with cumulative distribution functions (cdf's) instead of densities. Extracting a density from the simulation requires taking a numerical derivative, i.e., choosing a bin size and computing a histogram. Using the cdf's avoids this.

In our conjecture (4) the probability measure E_N only depends on whether the geometry we are studying is chordal or radial. So we only need to do two simulations, one for the chordal cases and one for the radial cases. In each simulation we sample the Markov chain every 100 time steps. In the chordal case we generated 9×10^9 samples and in the radial case 11×10^9 samples. For each sample and each domain D we test if $1_D(\omega) = 1$. When it does we use that sample in the computation of the cdf of the boundary density for that domain. The probability that $1_D(\omega) = 1$ depends on N and on the domain. In our simulations it ranges from $\frac{1}{3}\%$ to 2%.

The first domain we consider is a horizontal strip of height 1. For this domain there are no lattice effects since the entire boundary is horizontal. We consider both a chordal case and a radial case. In the chordal case the strip is $\{z : 0 < \text{Im}(z) < 1\}$. The SAW starts at the origin and ends on the upper boundary. In the radial case the strip is $\{z : -1/4 < \text{Im}(z) < 3/4\}$. The SAW starts at the origin and can end on either boundary. The conjectured density for the chordal case was tested by simulation in [3]. Here we are primarily interested in using these domains to test our conjecture (4) that uses the fixed length ensemble for the simulation, especially the value of the power p .

In figure 2 we plot six curves. Two curves are the cdf's computed using SLE partition functions for the chordal and radial cases. The other four curves are simulation cdf's for the chordal and radial cases. In each case we have two simulations, one with the power p given by (5) and one with $p = 0$. The curves from the SLE prediction and the curves from simulations with the correct value of p are indistinguishable on this plot, and so it appears there are only four curves in the figure. The maximum difference between these curves is given in table 1. It is on the order of 10^{-4} in the chordal case and 1.5×10^{-4} in the radial case. The discrepancy for the curves with $p = 0$ is quite large for the radial strip. For the chordal strip it is smaller, but can still be clearly seen in the plot. The maxima of the differences for the $p = 0$ case is

| Domain | | $l(\theta)$ used ? | max of difference of cdf's (in thousandths) |
|--------------------|---------|--------------------|--|
| Strip with $p = 0$ | chordal | | 26.90980 ± 0.63765 |
| Strip with $p = 0$ | radial | | 229.35605 ± 0.64829 |
| Strip | chordal | | 0.09842 ± 0.11619 |
| Strip | radial | | 0.15563 ± 0.15085 |
| Triangle | radial | yes | 0.05939 ± 0.08689 |
| Centered circle | radial | no | 3.16364 ± 0.07145 |
| Centered circle | radial | yes | 0.10997 ± 0.07793 |
| Off-center circle | radial | no | 2.26140 ± 0.09184 |
| Off-center circle | radial | yes | 0.07513 ± 0.08061 |
| Partial circle | chordal | no | 1.28211 ± 0.06962 |
| Partial circle | chordal | yes | 0.09512 ± 0.06158 |
| Tangent circle | chordal | no | 1.87370 ± 0.10155 |
| Tangent circle | chordal | yes | 0.18705 ± 0.10116 |

Table 1: For each domain the last column is the maximum of the absolute value of the difference between two cdf's. One cdf is computed using the SLE partition function prediction for the density. The other is from the SAW simulation. The middle column indicates if the lattice effect $l(\theta)$ is corrected for.

also given in the table.

We can estimate the power p by minimizing the difference between the boundary density computed by simulation using the conjecture (4) and the SLE prediction for the boundary density. We use the two strip geometries described above and minimize the L^2 norm of the difference between the densities. Our simulations to estimate the power p are separate from the simulations to compute the boundary densities. We use SAW's with 100,000 steps. For the chordal geometry we generated approximately 8 million samples and for the radial geometry approximately 10 million samples. By samples we mean SAW's for which $1_D(\omega) = 1$. In the chordal case the conjectured exact value is $p = -3/4 = -0.75$ and from the simulations we find the minimum difference is when $p = -0.751874$, a difference of 0.25%. In the radial case the conjectured exact value is $p = -61/48 = -1.27083\bar{3}$ and from the simulations we find -1.269917 , a difference of 0.07%.

Next we consider an equilateral triangle centered at the origin whose vertices have polar angles of 0, 120 and 240. The side corresponding to polar angles in $[120, 240]$ is vertical and the sides corresponding to $[0, 120]$ and $[240, 360]$ are at 30 degrees with respect to the lattice directions. So two of the sides will have the same value of $l(\theta)$ while the third side has a different value. This geometry gives an extreme example of the lattice effects. We simulate the ensemble with the weight factor $W(\omega)$ which does not correct for the lattice effects. We find that the probabilities for hitting the sides corresponding to $[0, 120]$, $[120, 240]$, $[240, 360]$ are

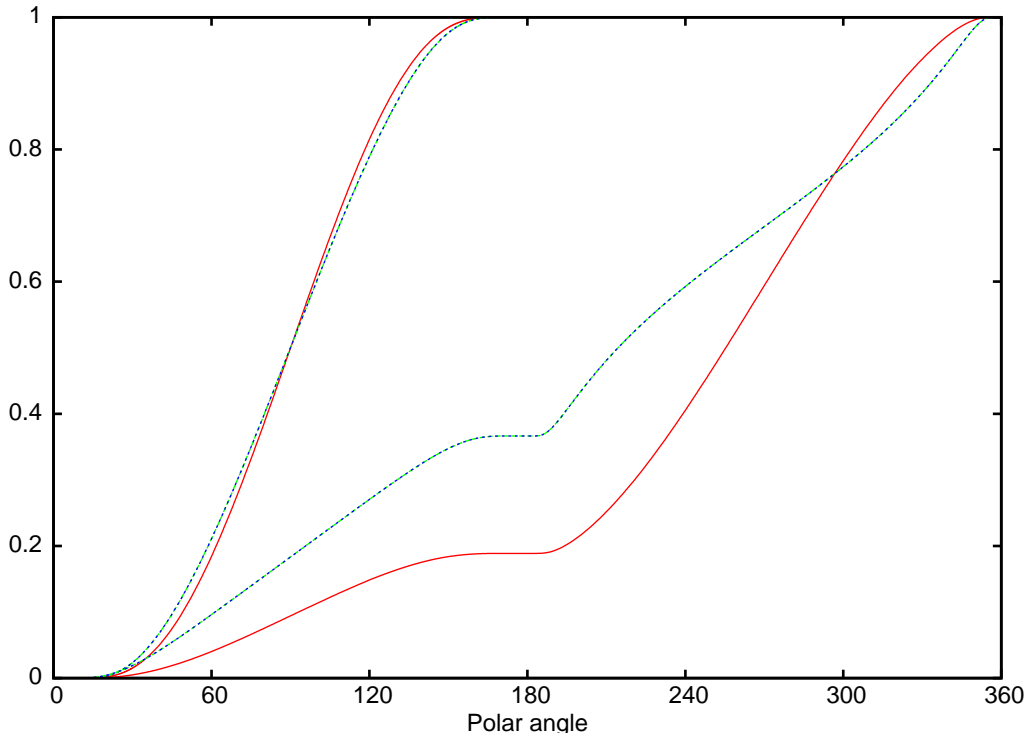


Figure 2: Comparison of cdf's from simulations and theory for chordal strip (polar angle ranges over $[0, 180]$) and radial strip (polar angle ranges over $[0, 360]$). The solid curves are simulations using $p = 0$. The overlying dashed curves are the simulations with the correct p and the SLE prediction.

0.387375, 0.225173, 0.387452 respectively. The ratio of the smaller probability to the average of the other two probabilities is 0.581221. This should be compared with the ratio of the two values of the lattice effect function which is $l(0)/l(30) = 0.581281$. In figure 3 we plot the cdf from our simulation. The smaller probability of hitting the vertical side is clearly seen. The two horizontal lines are at the heights predicted by the lattice effect function. For this geometry the only lattice effect should be to make the probabilities of hitting the three different sides unequal. Given that you hit a particular edge, the distribution along that edge should be the same for the three edges. So we can remove the lattice effect by looking at the polar angle of the endpoint mod 120. We compute the cdf of this random variable. In the inset in figure 3 we show this cdf minus the SLE partition function prediction for this cdf. This difference is quite small, on the order of 5×10^{-5} . The maximum of the difference is given in table 1.

The next domain we consider is a unit disc centered at the origin. As always, the SAW starts at the origin. The SLE partition function prediction is just that the density is uniform. The deviation from this is entirely due to lattice effects. The boundary density will have a period of 90 degrees, so we take the polar angle of the endpoint of the walk mod 90. In figure 4 we plot

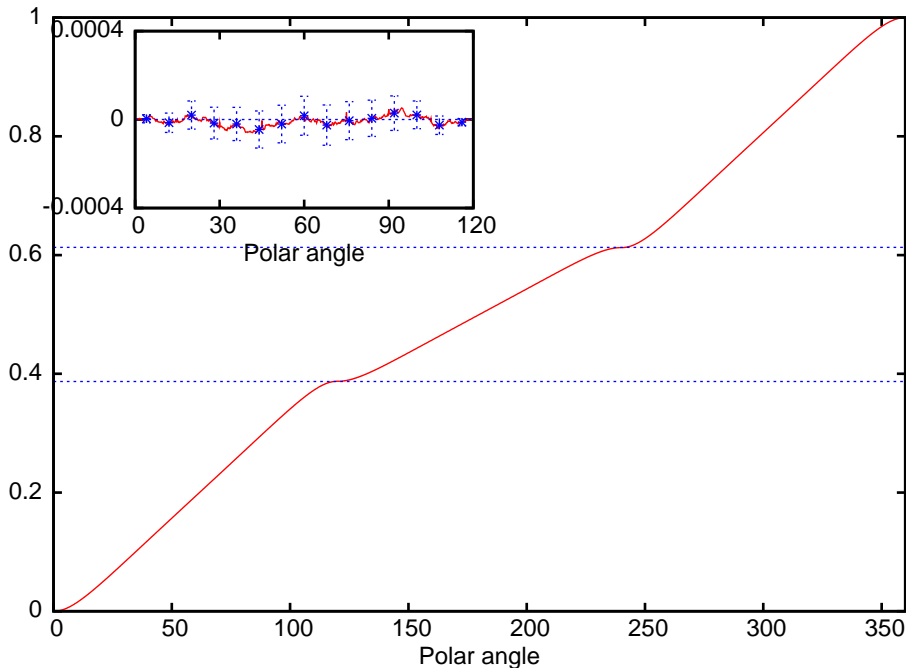


Figure 3: Simulation cdf for the equilateral triangle. The inset shows the difference of the simulation cdf and the theoretical cdf when the polar angle is reduced mod 120 to remove the lattice effects.

two curves. Both are the cdf from the simulation minus the cdf of the uniform distribution. In one we use the weight factor $W(\omega)$ which does not include the lattice effect correction, and in the other we use the weight factor $\hat{W}(\omega)$ which does include the correction. The sine-like curve is for the simulation without the lattice correction. The difference is small, on the order of 0.003, but clearly not zero. The flat curve is the difference when we do include the lattice effect correction in the simulation. The size of this difference is a test of our prediction for the lattice effect correction. The difference is extremely small, on the order of 10^{-4} . The maximum of the difference with and without the lattice correction is given in table 1.

Our last three simulations involve geometries for which the conjectured density from (5) is non-trivial and the lattice function $l(\theta)$ enters in a non-trivial way. In the first of these geometries the domain is a unit disc centered at $3/4$. We consider SAW's that start at the origin and end on the arc of the circle. As before we consider the difference between the cdf from the simulation and the cdf predicted by SLE partition functions. As before we consider two cases, one using the weight $W(\omega)$ and one using the weight $\hat{W}(\omega)$. We refer to this geometry as the “off-center circle” and give the maximum of the difference of the cdf's in table 1. As in the previous geometry the difference when we do not correct for the lattice effect is clearly non-zero, while it is zero within the errors in the simulation when we do correct for the lattice effects.

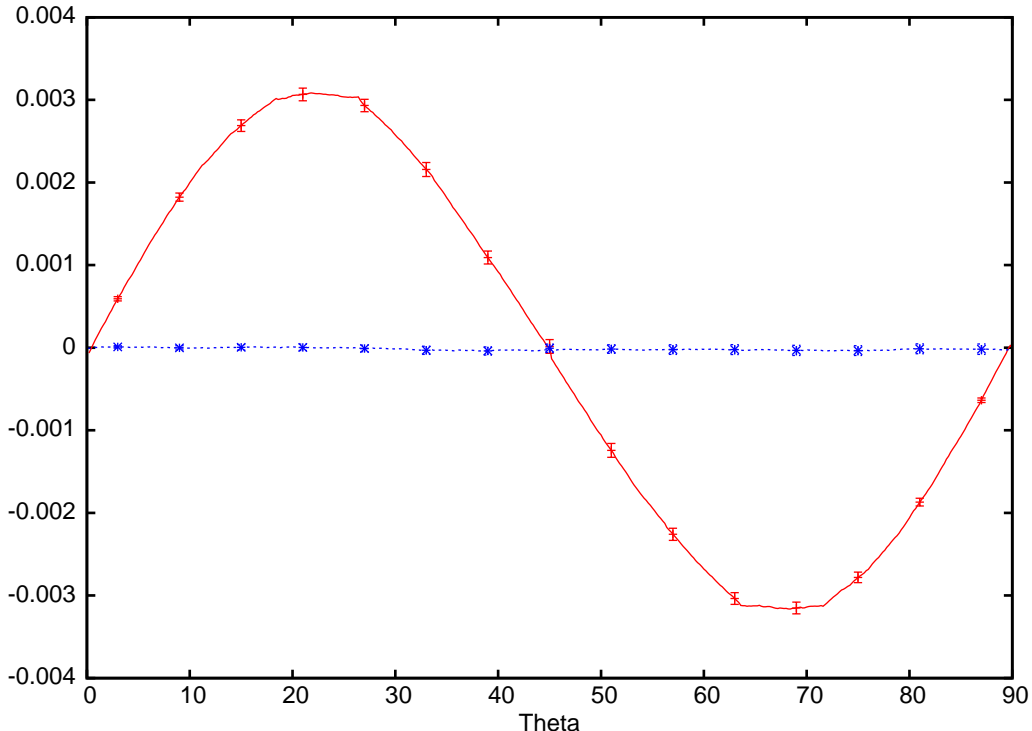


Figure 4: Difference of cdf's from simulations and theory for disc with origin at the center. The sine-like curve is for the simulation which does not correct for the lattice effects; the flat curve is for the simulation that does correct.

In the next geometry the domain is the intersection of the unit disc centered at $-3i/4$ and the upper half plane. So the domain is bounded by the real axis and the portion of the unit circle centered at $-3i/4$ that lies above the real axis. We consider SAW's that start at the origin and end on the arc of the circle. This geometry is called “partial circle” in the table. In the final geometry the domain is a unit disc centered at i . So the real axis is tangent to the disc at the origin. We consider SAW's starting at the origin and ending on the upper half of the boundary. So the polar angle with respect to the origin ranges from 45 to 135 degrees. This geometry is called “tangent circle” in the table. For both of these geometries the maxima of the differences is given in table 1. They are clearly non-zero when we do not correct for the lattice effects, while they are zero within the errors in the simulation when we do correct for the lattice effects.

5 Conclusions

We have studied SAW's in a bounded domain D which start at a fixed point (either in the interior or on the boundary) and end at an unconstrained point on the boundary. The dilation

ensemble of SAW's consists of all SAW's starting at the origin with the property that they can be scaled to give a curve inside our domain D which ends on the boundary of D . It can be thought of as interpreting the constraint that a SAW ends on the boundary of D by thickening the boundary. We weight a SAW ω by the usual weight of $\mu^{-|\omega|}$ times two factors. The factor $W(\omega)$, given by (3), accounts for the varying thickness of the boundary. The other factor of $1/l(\theta)$ accounts for the local lattice effect near the endpoint of the SAW that persists in the scaling limit.

We have conjectured that the scaling limit of the dilation ensemble is related to the limit as $N \rightarrow \infty$ of the uniform measure on SAW's with N -steps conditioned on the event that when the SAW is scaled so that it ends on the boundary of D , the SAW lies entirely in D . We have used our conjecture to simulate the SAW in several bounded domains and compared the distribution of the endpoint of the SAW on the boundary with the SLE partition function prediction of this density. We find excellent agreement. This supports our conjectured relationship between the dilation ensemble and the uniform probability measure on SAW's of a fixed length, the conjecture for the lattice effects that persist in the scaling limit and the SLE partition function predictions for the boundary density. Note our simulations only looked at the boundary density of the endpoint of the SAW. By using the SLE prediction for the boundary density and various explicit predictions about chordal and radial SLE, one can make explicit predictions about the SAW curve inside D and use our conjecture to test them. We have not carried out such simulations.

A Computation of SLE partition functions

In this appendix we give the analytic computations of the boundary density for the various domains. We use $\rho(\cdot)$ to denote the boundary density with respect to arc length (or a constant multiple of arc length) along C . In all cases the SAW starts at the origin. The constant c in the following is determined by the requirement that ρ is a probability density.

A.1 Strip - chordal

The domain is a strip of height 1 with the origin on the lower boundary. We are interested in the ensemble of SAW's in the strip that start at the origin and end at some point on the upper boundary of the strip. We parametrize the upper boundary by $x + i$ where $-\infty < x < \infty$. A straightforward application of (5) yields the boundary density with respect to dx .

$$\rho(x) = c [\cosh(\pi x/2)]^{-5/4}$$

A.2 Strip - radial

The domain is a horizontal strip of height 1, with the origin at a height h above the bottom boundary. So the domain is $\{z : -h \leq \text{Im}(z) \leq 1 - h\}$. We consider the ensemble of SAW's in

this strip that start at the origin, and end at a point on either the top or bottom boundary of the strip. We parametrize the lower boundary by $x - ih$ and the upper boundary by $x + (1 - h)i$ where $-\infty < x < \infty$. Then the boundary density with respect to dx is

$$\rho(x + iy) = \begin{cases} c [\cosh(\pi x) - \cos(\pi h)]^{-5/8} & \text{if } y = -h \\ c [\cosh(\pi x) + \cos(\pi h)]^{-5/8} & \text{if } y = 1 - h \end{cases}$$

A.3 Triangle

We use the Schwarz-Christoffel mapping

$$F(z) = \int_z^\infty (w + 1)^{-2/3} (w - 1)^{-2/3} dw$$

which maps the upper half plane onto an equilateral triangle. It sends $-1, 1, \infty$ to the vertices, and some simple substitutions show it sends $-3, 0, 3$ to the midpoints of the three sides. To find the pre-image of the center of the triangle, note that the center of triangle is the unique point fixed by rotations about the center. These rotations are the conformal automorphisms of the triangle that permute the vertices. So they correspond to conformal automorphisms of the half plane that permute $-1, 1$ and ∞ . Such Möbius transformations fix $i\sqrt{3}$, so $F(i\sqrt{3})$ is the center of the triangle.

A simple application of (5) shows that for SAW's in the half plane starting at $i\sqrt{3}$, the boundary density along the real axis is proportional to $(x^2 + 3)^{-5/8}$. By symmetry it is enough to find the boundary density for the triangle between the midpoint of one edge and a vertex. We consider $F(3, \infty)$. (For $|z| \geq 3$, $F(z)$ can be computed numerically very quickly by a power series expansion.) Let l_0 be the length of the edges in the triangle. We define $l = l(x)$ by

$$\frac{2l(x)}{l_0} = \frac{F(x)}{F(3)}$$

Then $l(x)$ is the distance from $F(x)$ to the vertex $F(\infty)$. Applying (5) we find the boundary density with respect to dl :

$$\rho(l) = c \frac{|F'(x)|^{-5/8}}{(x^2 + 3)^{5/8}} = c \frac{(x^2 - 1)^{5/12}}{(x^2 + 3)^{5/8}}$$

A.4 Off-center circle

The domain D is a unit disc centered at $a + ib$ where $|a + ib| < 1$ so that the origin is inside the disc. Let ϕ be the polar angle of a point on the boundary with respect to the center at $a + ib$. So ϕ is proportional to arc length along the boundary. An application of (5) with a Moibius transformation yields the boundary density with respect to $d\phi$.

$$\rho(\phi) = c [1 + a^2 + b^2 + 2a \cos \phi + 2b \sin \phi]^{-5/8}$$

A.5 Partial circle - chordal

We consider the unit disc centered at b where b is real and $|b| < 1$. So part of the disc lies below the real axis. We take the domain to be the intersection of this disc with the upper half plane. We consider SAW's in this domain that start at the origin and end on the arc of the circle above the real axis.

The circle intersects the real axis at $\pm d$ with $d = \sqrt{1 - b^2}$. The map $-(z + d)/(z - d)$ maps the domain to the wedge $0 < \arg(z) < \beta$ where $\tan \beta = -\sqrt{1 - b^2}/b$. So if we let

$$f(z) = \left[-\frac{z + d}{z - d} \right]^{\pi/\beta}$$

then f maps the domain to the upper half plane and sends 0 to 1. The endpoint of the walk is mapped to a point on the negative real axis.

An easy application of (5) shows that for the SAW in the upper half plane starting at 1 and ending at x on the negative real axis, the boundary density is proportional to $(1 - x)^{-5/4}$. So applying (5) to the map f shows that the boundary density with respect to $d\phi$ is

$$\rho(\phi) = c \left[\frac{|z + d|^{-1 + \pi/\beta}}{|z - d|^{1 + \pi/\beta}} \right]^{5/8} \frac{1}{(1 - f(z))^{5/4}}$$

where $z = ib + e^{i\phi}$.

A.6 Tangent circle - chordal

The domain is a disc of radius 1 centered at i so it is tangent to the real axis at the origin. Let ϕ be the polar angle with respect to i , so ϕ is proportional to arc length along the boundary. We condition on the event that the walk stays in this disc and ends on the upper half of the circle bounding the disc, i.e., the arc of the boundary where $0 \leq \phi \leq 180$.

The boundary density for the upper half plane when the SAW starts at the origin is $x^{-5/4}$. So using a Möbius transformation to map the disc to the half plane, the formula (5) gives the density with respect to $d\phi$:

$$\rho(\phi) = c |1 - \cos \phi + \sin \phi|^{-5/4} (1 - \cos \phi)^{5/8}$$

References

- [1] N. Clisby, Efficient implementation of the pivot algorithm for self-avoiding walks, J. Statist. Phys. **140**, 349-392 (2010). Archived as arXiv:1005.1444v1 [cond-mat.stat-mech].
- [2] H. Duminil-Copin, S. Smirnov, The connective constant of the honeycomb lattice equals $\sqrt{2 + \sqrt{2}}$, Preprint, 2010. Archived as arXiv:1007.0575v1 [math-ph].

- [3] B. Dyhr, M. Gilbert, T. Kennedy, G. Lawler, and S. Passon, The self-avoiding walk in a strip, *J. Statist. Phys.* **144**, 1-22 (2011). Archived as arXiv:1008.4321v2 [math.PR].
- [4] T. Kennedy, Transforming fixed-length self-avoiding walks into radial $SLE_{8/3}$, to appear in *J. Statist. Phys.* (2011). Archived as arXiv:1102.4082v1 [math.PR].
- [5] T. Kennedy, G. Lawler, Lattice effects in the scaling limit of the two-dimensional self-avoiding walk, preprint (2011). Archived as arXiv:1109.3091v1 [math.PR].
- [6] G. Lawler, Schramm-Loewner evolution, in *Statistical Mechanics*, S. Sheffield and T. Spencer, ed., IAS/Park City Mathematical Series, AMS, 231-295 (2009). Archived as arXiv:0712.3256v1 [math.PR].
- [7] G. Lawler, O. Schramm, and W. Werner, On the scaling limit of planar self-avoiding walk, *Fractal Geometry and Applications: a Jubilee of Benoit Mandelbrot, Part 2*, 339–364, *Proc. Sympos. Pure Math.* **72**, Amer. Math. Soc., Providence, RI, 2004. Archived as arXiv:math/0204277v2 [math.PR]
- [8] N. Madras and G. Slade, *The Self-Avoiding Walk*, Birkhäuser (1996).